ANZIAM J. 58(2017), 287–305
doi:10.1017/S1446181117000244

COVERAGE PERFORMANCE OF COGNITIVE RADIO NETWORKS POWERED BY RENEWABLE ENERGY

XIAOLONG CHEN ✉ [1], XIANGBO MENG [2], XIAOSHI SONG [2] and CHUN SHAN [3]

(Received 19 October, 2016; accepted 17 November, 2016; first published online 24 May 2017)

Abstract

We analyse the coverage performance of cognitive radio networks powered by renewable energy. Particularly, with an energy harvesting module and energy storage module, the primary transmitters (PTs) and the secondary transmitters (STs) are assumed to be able to collect ambient renewables, and store them in batteries for future use. Upon harvesting sufficient energy, the corresponding PTs and STs (denoted by eligible PTs and STs) are then allowed to access the spectrum according to their respective medium access control (MAC) protocols. For the primary network, an Aloha-type MAC protocol is considered, under which the eligible PTs make independent decisions to access the spectrum with probability ρ_p. By applying tools from stochastic geometry, we characterize the transmission probability of the STs. Then, with the obtained results of transmission probability, we evaluate the coverage (transmission nonoutage) performance of the overlay CR network powered by renewable energy. Simulations are also provided to validate our analysis.

2010 *Mathematics subject classification*: 60D05.

Keywords and phrases: cognitive radio, opportunistic spectrum access, stochastic geometry, Poisson point process, coverage probability, renewable energy.

1. Introduction

Explosive mobile data demands have stimulated a significant growth of energy consumption in mobile networks, and thereby have led to a considerable rise in carbon footprints. To reduce the energy cost and alleviate the carbon emissions, the concept of renewable energy harvesting [4, 6, 9, 10, 12] has received substantial attention as an effective approach to increase the energy efficiency of mobile networks. In particular, powered by ambient renewables (such as solar and wind), the mobile networks are

[1] Jinhua Polytechnic, Jinhua, 321017, China; e-mail: xlycxl@126.com.
[2] School of Computer Science and Engineering, Northeastern University, Shenyang 110819, China; e-mail: mengxiangbo.neu@gmail.com, songxiaoshi@cse.neu.edu.cn.
[3] School of Accountancy, Guangdong Polytechnic Normal University, Guangdong 510665, China; e-mail: mmc518@126.com.

envisioned to be not only environmentally friendly but also self-sustaining. Further, with stand-alone renewable energy harvesters, it is feasible to deploy the wireless network without relying on the infrastructure of the power line.

Beside maximizing energy efficiency, another important issue in the design of wireless networks is to maximize the spectrum efficiency, due to the explosive growth of mobile devices and data-hungry applications. Particularly, the inefficient use of the limited spectrum resources is considered to be the main bottleneck for improving the performance of wireless networks. To tackle such difficulty, concepts of cognitive radio (CR) [25, 29] and opportunistic spectrum access (OSA) [20–31] are proposed as promising approaches to improve the spectrum efficiency. The basic idea of OSA in CR networks is to enable the unlicensed secondary users to access the licensed spectrum by utilizing the spectrum holes [22] available in the primary network. As such, with OSA, the unused spectrum in the primary network can be effectively exploited by the secondary users.

In this paper, we consider a renewable energy powered CR network to improve both the energy efficiency and spectral efficiency in the next generation wireless networks. Particularly, with renewable energy harvesting, the PTs and STs are assumed to be self-sustained, which thereby potentially enables a perpetual operation of the CR network without the need for external power supply. On the other hand, the OSA allows the dynamic access of STs, which can effectively improve the spectrum efficiency. Note that in general, such a large-scale renewable energy powered CR network can be considered as an attractive alternative for various types of future mobile networks, such as ultra-dense cellular networks [30], device-to-device (D2D) networks [32] and wireless caching networks [24].

Renewable energy powered CR networks have been widely studied in the literature [3–18]. Park et al. [17, 18] investigated the maximum throughput of renewable energy powered secondary transmitter, under the assumptions of perfect spectrum sensing and imperfect spectrum sensing, respectively. Pappas et al. [16] studied the maximum stable throughput region for a simple cognitive radio network with the primary transmitter powered by ambient renewables. Yin et al. [27, 28] investigated the optimal sensing and cooperation strategies of secondary users powered by renewable energy to maximize the achievable throughput of the CR network. Also, Chung et al. [3] investigated the optimal sensing duration and energy detectors sensing threshold to maximize the average throughput of the CR network powered by renewable energy. Note that in the literature [3–18], the studied CR networks contained only one primary link and one secondary link, therefore, the CR networks were simple and relatively small. Further, it is worth noting that the impact of the locations of PTs and STs were not taken into consideration in these papers.

In this paper, unlike previous work [3–18], we consider a large-scale overlay CR network powered by renewable energy, and assume that the locations of PTs and STs are distributed as Poisson point processes. Both the PTs and STs are assumed to be able to collect ambient renewables and store them in batteries for future use. With sufficient energy stored in the batteries, the corresponding PTs and STs (denoted by eligible PTs and STs) are then allowed to access the spectrum according to their respective medium access control (MAC) protocols. For the primary network, an Aloha-type MAC protocol [2] is considered, under which the eligible PTs make independent decisions to access the spectrum with probability ρ_p. For the secondary network, a threshold-based opportunistic spectrum access (OSA) scheme, namely, the primary receiver assisted (PRA) protocol is investigated. Under this scheme, an eligible ST is allowed to access the spectrum, only when the maximum signal power of the received beacons sent from the active primary receivers (PRs) is lower than a predefined threshold N_{ra}. By applying tools from random walk theory [5] and stochastic geometry [1], the transmission probabilities of PTs and STs are analysed under the assumption that the battery capacity is infinite. Further, based on the obtained results of transmission probability, the coverage (transmission nonoutage) performance in the overlay CR network powered by renewable energy is characterized. Simulations are also provided to validate our analysis.

The remainder of this paper is organized as follows. The system model is described in Section 2 and the transmission probabilities of PTs and STs are characterized in Section 3. The coverage performance of the primary and secondary networks is analysed in Sections 4 and 5, respectively. Simulation results are presented in Section 6. Finally, we conclude the paper in Section 7.

2. Model and metric

2.1. System model We consider an overlay CR network in which two mobile ad hoc networks, namely, the primary network and the secondary network coexist and share the same spectrum on $\mathbb{R}^2$. The PTs are licensed users with a higher priority to access the spectrum, while the STs are allowed to transmit, only if they are detected to be in the spatial holes of the primary network. The locations of the PTs and STs are assumed to follow two independent homogeneous Poisson point processes (HPPPs) with density μ_0 and λ_0, respectively. For each PT, the intended PR is located at a distance d_p away in a random direction. Similarly, for each ST, the intended secondary receiver (SR) is located at a distance d_s away in a random direction. It should be noted that the locations of the PRs (or SRs) are not part of their respective transmitters' Poisson point processes (PPPs). Thus, the locations of the PRs and SRs follow two independent HPPPs with density μ_0 and λ_0, respectively.

We assume that time is slotted. In each time slot with an energy harvesting module and energy storage module, the PTs and STs are assumed to be able to collect ambient renewables and store them in batteries for future use. Particularly, with t as the slot index, the amount of renewable energy harvested by the PT and ST located at arbitrary positions, $\mathbf{x} \in \mathbb{R}^2$ and $\mathbf{y} \in \mathbb{R}^2$ in the tth time slot, can be represented by a nonnegative random variable $Z_t^p(\mathbf{x})$ or $Z_t^s(\mathbf{y})$, respectively. The corresponding expectation and variance are given by

$$\mathbf{E}[Z_t^p(\mathbf{x})] = \nu_e^p, \tag{2.1}$$

$$\mathbf{Var}[Z_t^s(\mathbf{x})] = \delta_e^p,$$

https://doi.org/10.1017/S1446181117000244 Published online by Cambridge University Press

and

$$\mathbf{E}[Z_t^s(\mathbf{y})] = \nu_e^s,$$

$$\mathbf{Var}[Z_t^s(\mathbf{x})] = \delta_e^s,$$

respectively. Further, we assume that the PRs and SRs are powered by some reliable energy sources.

The primary network is assumed to employ an Aloha-type MAC protocol [2] such that the PTs make independent decisions to access the spectrum with probability ρ_p. For the secondary network, the PRA protocol [20] is employed, such that the STs are allowed to transmit only if they are detected to be in the resulting spatial spectrum holes of the primary network. Particularly, given $M_t^{ra}(\mathbf{y})$ as the maximum received beacon power at an arbitrary ST located at position $\mathbf{y}$ in the tth time slot, the corresponding ST is allowed to launch the transmission only if $M_t^{ra}(\mathbf{y})$ is lower than a predefined threshold N_{ra}.

Let $\mathbf{B}_p$ and $\mathbf{B}_s$ denote the battery capacities for PTs and STs, respectively. Further, let P_p and P_s denote the transmitted power of the PTs and STs, respectively. Then, given $S_t^p(\mathbf{x})$ and $S_t^s(\mathbf{y})$ as the battery levels of PT and ST located at positions $\mathbf{x} \in \mathbb{R}^2$ and $\mathbf{y} \in \mathbb{R}^2$ in the tth slot, we obtain

$$S_t^p(\mathbf{x}) = \min\,(S_{t-1}^p(\mathbf{x}) + Z_t^p(\mathbf{x}) - P_p \cdot \mathcal{G}_t^p, \mathbf{B}_p), \tag{2.2}$$

and

$$S_t^s(\mathbf{y}) = \min\,(S_{t-1}^s(\mathbf{y}) + Z_t^s(\mathbf{y}) - P_s \cdot \mathcal{G}_t^s, \mathbf{B}_s), \tag{2.3}$$

where

$$\mathcal{G}_t^p = \mathcal{X}_t^p \cdot \mathbf{1}_{S_{t-1}^p(\mathbf{y}) \geq P_p}, \tag{2.4}$$

and

$$\mathcal{G}_t^s = \mathbf{1}_{S_{t-1}^s(\mathbf{y}) \geq P_s} \cdot \mathbf{1}_{M_t^{ra}(\mathbf{y}) \leq N_{ra}}, \tag{2.5}$$

with $\mathbf{1}_{\mathcal{A}}$ as the indicator function with respect to event $\mathcal{A}$, and $\mathcal{X}_p$ as a Bernoulli random variable with probability

$$P(\mathcal{X}_t^p = 1) = \rho_p.$$

It is worth noting that for the primary network, due to the spatial stationarity of the energy-arrival process $Z_t^p(\mathbf{x})$, the locations of the active PTs (PRs) in the tth time slot follow a HPPP with density $\mu_t^p = \eta_t^p \mu_0$ under the Aloha-type MAC protocol, where

$$\eta_t^p = \mathbb{E}[\mathcal{X}_t^p \cdot \mathbf{1}_{S_{t-1}^p(\mathbf{y}) \geq P_p}]. \tag{2.6}$$

For the secondary network, however, unlike the position-independent thinning in the primary network, the access probabilities of the STs under the PRA protocol are position-dependent. As such, the point process formed by the active STs under the PRA protocol does not follow a HPPP. In fact, under the PRA protocol, the access probability of each ST is a function of the realization of active PRs (PTs). Nevertheless, due to the fact that the active PRs (PTs) are homogeneously Poisson

https://doi.org/10.1017/S1446181117000244 Published online by Cambridge University Press

distributed, and due to the spatial stationarity of the energy-arrival process $Z_t^p(\mathbf{y})$, the access probabilities of all STs are identically distributed. Therefore, the randomly thinned point process formed by the active STs under the PRA protocol is stationary on $\mathbb{R}^2$. Particularly, under the PRA protocol, the density of the point process formed by the active STs in the tth time slot is given by $\mu_t^s = \eta_t^s \lambda_0$, where

$$\eta_t^s = \mathbb{E}[\mathbf{1}_{S_{t-1}^s(\mathbf{y}) \geq P_s} \cdot \mathbf{1}_{M_t^{ra}(\mathbf{y}) \leq N_{ra}}]. \tag{2.7}$$

The propagation channel is modelled as the combination of the small-scale Rayleigh fading [19] and the large-scale path-loss given by $g(d) = hd^{-\alpha}$, where h denotes the exponentially distributed power coefficient with unit mean, d denotes the propagation distance and α denotes the path-loss exponent [26]. For the sake of simplicity, we ignore the thermal noise in the regime of interest and simply focus on the received signal-to-interference ratio (SIR) as in the articles [13]–[23]. We further denote θ_p and θ_s as the SIR targets for primary and secondary networks, respectively.

2.2. Performance metric Three performance metrics are studied in this paper: the transmission probability, the coverage probability and the spatial throughput, which are specified as follows.

2.2.1 *Transmission probability.* Assuming infinitely backlogged and packetized data, based on equations (2.6)–(2.7), the transmission probability of PTs and STs is defined as

$$\eta^p = \lim_{n\to\infty} \frac{1}{n} \sum_{t=1}^{n} \eta_t^p, \tag{2.8}$$

and

$$\eta^s = \lim_{n\to\infty} \frac{1}{n} \sum_{t=1}^{n} \eta_t^s,$$

respectively.

2.2.2 *Coverage probability.* The coverage probability, also known as the transmission nonoutage probability, is defined as the probability that a (primary or secondary) receiver succeeds in decoding the received data packets from its corresponding (primary or secondary) transmitter. In particular, given the primary or secondary receiver SIR, denoted by SIR_p and SIR_s, respectively, and the corresponding SIR targets, θ_p and θ_s, the coverage probability in the primary or secondary network is defined as

$$\tau_p = P\{\mathrm{SIR}_p \geq \theta_p\}, \quad \text{and} \quad \tau_s = P\{\mathrm{SIR}_s \geq \theta_s\}.$$

2.2.3 *Spatial throughput.* The spatial throughput of the primary (secondary) network is the expected spatial density of successful primary (secondary) transmissions, which are donated by C_p and C_s, respectively, defined as

$$C_p = \mu_p \tau_p, \quad \text{and} \quad C_s = \lambda_s \tau_s,$$

where $\mu_p = \eta^p \mu_0$ and $\lambda_s = \eta^s \lambda_0$.

https://doi.org/10.1017/S1446181117000244 Published online by Cambridge University Press

3. Transmission probability with infinite battery capacity

In this section, assuming that the PTs and STs are each equipped with a battery of infinite capacity, we characterize the transmission probabilities η^p and η^s, respectively. Particularly, based on equations (2.2)–(2.3), by letting $\mathbf{B} \to \infty$, we obtain

$$S_t^p(\mathbf{x}) = S_{t-1}^p(\mathbf{x}) + Z_t^p(\mathbf{x}) - P_p \cdot \mathcal{G}_t^p, \tag{3.1}$$

and

$$S_t^s(\mathbf{y}) = S_{t-1}^s(\mathbf{y}) + Z_t^s(\mathbf{y}) - P_s \cdot \mathcal{G}_t^s, \tag{3.2}$$

where $\mathcal{G}_t^p$ and $\mathcal{G}_t^s$ are defined in equations (2.4) and (2.5), respectively. Then, based on equations (3.1)–(3.2), we characterize the transmission probability η^p and η^s of PTs and STs in the following two theorems.

Theorem 3.1. *For an overlay* CR *network powered by renewable energy, assuming that the* PTs *are each equipped with a battery of infinite capacity, the transmission probability η^p of* PTs *under an Aloha-type* MAC *protocol with probability ρ_p is given by*

$$\eta^p = \min\left(\rho_p, \frac{\nu_e^p}{P_p}\right). \tag{3.3}$$

Proof. See Appendix A. □

Remark 3.2. Based on Theorem 3.1, the expected spatial density of the active PTs (PRs) can be immediately obtained as

$$\mu_p = \min\left(\mu_0\rho_p, \mu_0\frac{\nu_e^p}{P_p}\right). \tag{3.4}$$

Theorem 3.3. *For an overlay* CR *network powered by renewable energy, assuming that the* PTs *and* STs *are each equipped with a battery of infinite capacity, the transmission probability η^p of* STs *under the* PRA *protocol is given by*

$$\eta^s = \min\left(Q_{ra}, \frac{\nu_e^s}{P_s}\right), \tag{3.5}$$

where

$$Q_{ra} = \exp\left\{-2\pi\mu_p\frac{\Gamma(2/\alpha)(P_p/N_{ra})^{2/\alpha}}{\alpha}\right\}.$$

Proof. Based on the article [20], by applying a similar approach as in the proof of Theorem 3.1, equation (3.4) is immediately obtained. □

Remark 3.4. Based on Theorem 3.1, the expected spatial density of the active STs can be obtained as

$$\lambda_s = \min\left(\lambda_0 Q_{ra}, \lambda_0\frac{\nu_e^s}{P_s}\right).$$

In the next two sections, based on Theorems 3.1 and 3.3, we study the coverage probabilities of the primary and secondary networks, respectively, under the proposed PRA protocol.

https://doi.org/10.1017/S1446181117000244 Published online by Cambridge University Press

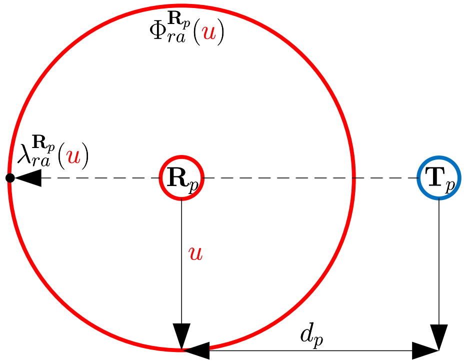

FIGURE 1. Conditional distribution of active STs under the PRA protocol.

4. Coverage probability in a primary network with infinite battery capacity

4.1. Conditional distribution of active STs To analyse the coverage performance of the primary network, due to the stationarity of the point processes formed by the active primary and secondary users, we may focus on a typical PR at the origin denoted by $\mathbf{R}_p$ with its associated PT at a distance of d_p, denoted by $\mathbf{T}_p$. Then, by Slivnyak's theorem [7], in both cases of the PRA protocol, the locations of the rest of the active PRs/PTs follow a HPPP with density μ_p. For the secondary network, let $\Phi_{ra}^{\mathbf{R}_p}(u)$ be the point process formed by the active STs on a circle of radius u centred at $\mathbf{R}_p$ under the PRA protocol, as illustrated in Figure 1. Then, we characterize the conditional distribution of the active STs under the PRA protocol in the following lemma. Note that a point process $\mathcal{N}$ is *isotropic*, if its characteristics are invariant under rotation [21].

LEMMA 4.1. *For an overlay* CR *network with the* PRA *protocol, conditioned on a typical* PR *at the origin,* $\Phi_{ra}^{\mathbf{R}_p}(u)$ *is isotropic with respect to* $\mathbf{R}_p$ *with density* $\lambda_{ra}^{\mathbf{R}_p}(u)$*, given by*

$$\lambda_{ra}^{\mathbf{R}_p}(u) = \min\left(\lambda_0 Q_{ra}\mathcal{P}(u),\ \lambda_0 \frac{\nu_e^s}{P_s}\right), \tag{4.1}$$

where $\mathcal{P}(u) = (1 - e^{-N_{ra}u^{\alpha}/P_p})$.

PROOF. According to Song et al. [20, Theorem 3.1], without conditioning on a typical PR at the origin, the spatial opportunity for a ST on a circle of radius u or r centred at $\mathbf{R}_p$ under the PRA protocol, is given by Q_{ra}. Conditioned on a typical PR at the origin, due to the newly introduced interference constraint at the typical PR, the spatial opportunity for a ST on the same circle centred at $\mathbf{R}_p$ under the PRA protocol reduces to $Q_{ra}P(h \le N_{ra}u^{\alpha}/P_p)$, where h denotes an exponentially distributed random variable with unit mean. Based on this result, by applying a similar approach as in the proof of Theorem 3.1, it can be easily verified that $\Phi_{ra}^{\mathbf{R}_p}(u)$ is isotropic around $\mathbf{R}_p$ with density $\lambda_{ra}^{\mathbf{R}_p}(u)$ given by equation (4.1). Thus, this completes the proof of the lemma. □

https://doi.org/10.1017/S1446181117000244 Published online by Cambridge University Press

It is worth noting that under the PRA protocol, due to the threshold-based OSA, $\Phi_{ra}^{\mathbf{R}_p}(u)$ does not follow a HPPP. Furthermore, since the higher order statistics of $\Phi_{ra}^{\mathbf{R}_p}(u)$ are intractable, the coverage probability of the primary network under the PRA protocol, which depends on the Laplace transform of the aggregate interference from all active STs to the typical PR at the origin, is difficult to characterize exactly. To tackle this difficulty, similar to the articles [13–15, 20], we make the following approximations on the conditional distribution of the active STs, which will be verified later by simulations in Section 6.

Assumption 4.2. Under the PRA protocol, conditioned on a typical PR at the origin, $\Phi_{ra}^{\mathbf{R}_p}(u)$ follows a HPPP with density $\lambda_{ra}^{\mathbf{R}_p}(u)$ and is assumed to be independent from the point process formed by the active PTs.

Based on Assumption 4.2, we next characterize the coverage performance of the primary network under the PRA protocol in the following subsection.

4.2. Coverage probability with PRA protocol

Theorem 4.3. *For an overlay* CR *network with the* PRA *protocol, under Assumption 4.2, the coverage probability of the primary network is given by*

$$\tau_p^{ra} = \exp\left\{-\frac{2\pi^2}{\alpha\sin(2\pi/\alpha)}\theta_p^{2/\alpha}d_p^2\mu_p\right\} \times \exp\left\{-2\pi\lambda_0 Q_{ra}\int_0^{\zeta}(1-\varrho(u))\mathcal{P}(u)u\,du\right\} \times \exp\left\{-2\pi\lambda_0\frac{\nu_e^s}{P_s}\int_{\zeta}^{\infty}(1-\varrho(u))u\,du\right\},$$

where

$$\zeta = \left\{-\frac{P_p}{N_{ra}}\ln\left(1-\frac{\eta^s}{Q_{ra}}\right)\right\}^{1/\alpha},$$

and

$$\varrho(u) = \int_0^{N_{ra}u^{\alpha}/P_p} e^{-(\theta_p P_s g u^{-\alpha})/P_p d_p^{-\alpha}} \times \frac{e^{-g}}{1-e^{-(-N_{ra}u^{\alpha})/P_p}}\,dg.$$

Proof. See Appendix B. □

Remark 4.4. It is worth noting that under the PRA protocol, the point process formed by the active STs is isotropic around the typical PR at the origin. This is the key to an exact characterization of the coverage probability of the primary network, which is obtained in Theorem 4.3.

Remark 4.5. With Theorem 4.3, the spatial throughput of the primary network under the PRA protocol is given by $C_p^{ra} = \mu_p\tau_p^{ra}$.

https://doi.org/10.1017/S1446181117000244 Published online by Cambridge University Press

5. Coverage probability in a secondary network with infinite battery capacity

5.1. Conditional distributions of active PTs and STs To analyse the coverage performance of the secondary network, we focus on a typical SR at the origin, denoted by $\mathbf{R}_s$ with its associated ST at a distance d_s denoted by $\mathbf{T}_s$. Let $\Psi_{ra}^{\mathbf{T}_s}(r)$ be the point process formed by the active PRs on a circle of radius r centred at $\mathbf{T}_s$ under the PRA protocol. Then, the conditional distribution of the active PRs under the PRA protocol is characterized as follows.

Lemma 5.1. *For an overlay* CR *network with the* PRA *protocol, conditioned on a typical SR at the origin,* $\Psi_{ra}^{\mathbf{T}_s}(r)$ *follows a* HPPP *with density*

$$\psi_{ra}^{\mathbf{T}_s}(r) = \min\biggl(\mu_0 \rho_p \mathcal{P}(r),\ \mu_0 \frac{\nu_e^p}{P_p}\biggr), \tag{5.1}$$

where $\mathcal{P}(r) = (1 - e^{-N_{ra} r^{\alpha}/P_p})$.

Proof. Based on the work of Song et al. [20, Lemma 5.1], by applying a similar approach as in the proof of Lemma 5.1, it can be verified that $\Psi_{ra}^{\mathbf{T}_s}(r)$ follows a HPPP with density $\psi_{ra}^{\mathbf{T}_s}(r)$ as given by equation (5.1). □

Let $\Upsilon_{ra}^{\mathbf{T}_s}(r)$ be the point process formed by the active PTs on a circle of radius r centred at $\mathbf{T}_s$ under the PRA protocol. Then, based on Lemma 5.1, we characterize the conditional distribution of the active PTs under the PRA protocol in the following lemma.

Lemma 5.2. *For an overlay* CR *network with the* PRA *protocol, conditioned on a typical SR at the origin,* $\Upsilon_{ra}^{\mathbf{T}_s}(r)$ *follows a* HPPP *with density* $\mu_{ra}^{\mathbf{T}_s}(r)$*, which is upper-bounded by*

$$\mu_{ra}^{\mathbf{T}_s}(r) \le \min\biggl(\mu_0 \rho_p \mathcal{P}(r + d_p),\ \mu_0 \frac{\nu_e^p}{P_p}\biggr).$$

Proof. The conditional distribution of the active PTs is related to that of their corresponding active PRs located at a distance d_p away in random directions. From Lemma 5.1, by applying a similar approach as in the proof of Lemma 5.1, it can be verified that $\Upsilon_{ra}^{\mathbf{T}_s}(r)$ follows a HPPP with density $\mu_{ra}^{\mathbf{T}_s}(r)$, which is (in the worst case) upper-bounded by $\psi_{ra}^{\mathbf{T}_s}(r + d_p)$. □

The conditional distribution of the active PTs under the PRA protocol is illustrated in Figure 2(a).

For the secondary network, let $\Phi_{ra}^{\mathbf{T}_s}(r)$ be the point process formed by the active STs on a circle of radius r centred at $\mathbf{T}_s$ under the PRA protocol as illustrated in Figure 2(b). Then, based on Lemma 5.1, the conditional distribution of the active STs under the PRA protocol is characterized as follows.

https://doi.org/10.1017/S1446181117000244 Published online by Cambridge University Press

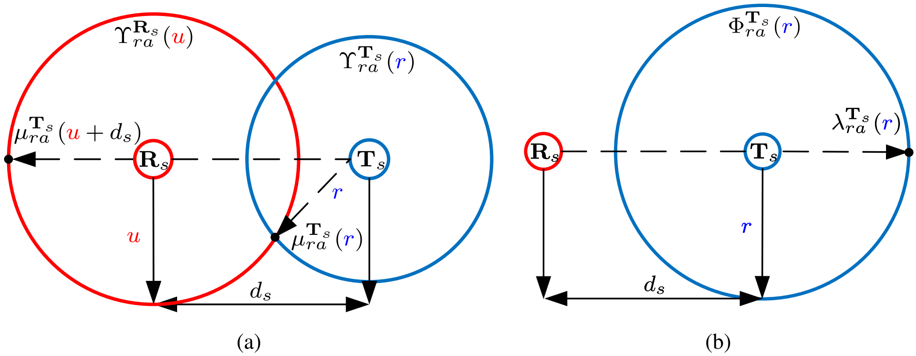

FIGURE 2. Illustration of the conditional distributions for (a) active PTs and (b) active STs, under the PRA protocol.

LEMMA 5.3. *For an overlay* CR *network with the* PRA *protocol, conditioned on a typical* SR *at the origin,* $\Phi_{ra}^{\mathbf{T}_s}(r)$ *is isotropic around* $\mathbf{T}_s$*, and the corresponding density denoted by* $\lambda_{ra}^{\mathbf{T}_s}(r)$*, is bounded by*

$$\mathcal{K} \le \lambda_{ra}^{\mathbf{T}_s}(r) \le \mathcal{D}, \tag{5.2}$$

where

$$\mathcal{D} = \min\left(\lambda_0 Q_{ra}\beta_{ra},\ \lambda_0 \frac{\nu_e^s}{P_s}\right), \quad \mathcal{K} = \min\left(\lambda_0 Q_{ra},\ \lambda_0 \frac{\nu_e^s}{P_s}\right),$$
$$\beta_{ra} = \exp\left\{\pi\mu_p \Gamma\left(\frac{2+\alpha}{\alpha}\right)\left(\frac{P_p}{2N_{ra}}\right)^{2/\alpha}\right\}.$$

PROOF. Based on the work of Song et al. [20, Lemma 5.3], by applying a similar approach as in the proof of Lemma 5.1, equation (5.2) is immediately obtained. Thus, this completes the proof of the lemma. □

Note that under the PRA protocol, similar to the primary network case, $\Phi_{ra}^{\mathbf{T}_s}(r)$ does not follow a HPPP. As a result, with only the first-order moment measures (average densities) of $\Phi_{ra}^{\mathbf{T}_s}(r)$ being obtained, the coverage probability of the secondary network under the PRA protocol is difficult to characterize exactly. To tackle this difficulty, we make the following assumption on the conditional distribution of the active STs, which will be verified by simulations in Section 6.

ASSUMPTION 5.4. Under the PRA protocol, conditioned on a typical SR at the origin, $\Phi_{ra}^{\mathbf{T}_s}(r)$ follows a HPPP with density $\lambda_{ra}^{\mathbf{T}_s}(r)$ and is assumed to be independent from the point process formed by the active PTs.

Based on Assumption 5.4, we characterize the coverage performance of the secondary network under the PRA protocols in the next two subsections.

https://doi.org/10.1017/S1446181117000244 Published online by Cambridge University Press

5.2. Coverage probability with PRA protocol Under the PRA protocol, let $\Upsilon_{ra}^{\mathbf{R}_s}(u)$ be the point process formed by the active PTs on a circle of radius u centred at $\mathbf{R}_s$ as illustrated in Figure 2(a). From Lemma 5.2, it follows that in general $\Upsilon_{ra}^{\mathbf{R}_s}(u)$ is a nonhomogeneous PPP. Let $\mu_{ra}^{\mathbf{R}_s}(u)$ be the average density of $\Upsilon_{ra}^{\mathbf{R}_s}(u)$. Then, we obtain the following lemma.

LEMMA 5.5. *Under the* PRA *protocol, conditioned on a typical* SR *at the origin, an upper bound on $\mu_{ra}^{\mathbf{R}_s}(u)$ is given by*

$$\mu_{ra}^{\mathbf{R}_s}(u) \le \min\Big(\mu_0 \rho_p \mathcal{P}(u + d_p + d_s), \mu_0 \frac{\nu_e^p}{P_p}\Big).$$

PROOF. Based on Lemma 5.2, the proof immediately follows from Figure 2(a) by observing that the highest density of $\mu_{ra}^{\mathbf{R}_s}(u)$ is $\mu_{ra}^{\mathbf{T}_s}(u + d_s)$. □

Now, we are ready to evaluate the coverage probability of the secondary network under the PRA protocol in the following theorem.

THEOREM 5.6. *For an overlay* CR *network with the* PRA *protocol, under Assumption 5.4, the coverage probability of the secondary network is lower-bounded by*

$$\begin{aligned}\tau_s^{ra} \ge{}& \exp\Big\{-\frac{2\pi^2}{\alpha \sin(2\pi/\alpha)} \theta_s^{2/\alpha} d_s^2 \mathcal{D}\Big\}\\ &\times \exp\Big\{-2\pi\mu_0\rho_p \int_0^{\varpi} \Big(\frac{1 - e^{-N_{ra}(u+d_p+d_s)^\alpha/P_p}}{1 + P_s u^\alpha/(\theta_s P_p d_s^\alpha)}\Big) u\, du\Big\}\\ &\times \exp\Big\{-2\pi\mu_0 \frac{\nu_e^p}{P_p} \int_{\varpi}^{\infty} \Big(\frac{1}{1 + P_s u^\alpha/(\theta_s P_p d_s^\alpha)}\Big) u\, du\Big\}, \end{aligned} \tag{5.3}$$

where

$$\varpi = \Big\{-\frac{P_p}{N_{ra}} \ln\Big(1 - \frac{\eta^p}{\rho_p}\Big)\Big\}^{1/\alpha} - d_p - d_s.$$

PROOF. Using Lemmas 5.3 and 5.5, the inequality given by equation (5.3) is readily obtained by applying a similar approach as in the proof of Theorem 4.3. □

REMARK 5.7. With Theorems 3.3 and 5.6, we establish a lower bound on the spatial throughput $C_s^{ra} = \lambda_s \tau_s^{ra}$ of the secondary network under the PRA protocol.

6. Numerical results

In this section, we present simulation results on the transmission probabilities and coverage probabilities of PTs and STs, respectively, to validate our analytical results. Throughout this section, unless specified otherwise, we set $\mu_p = 0.1$, $\lambda_0 = 0.1$, $P_p = 5$, $P_s = 2$, $d_p = d_s = 1$, $\theta_p = \theta_s = 3$ and $\alpha = 4$.

Figures 3 and 4 plot the analytical and simulation results on the transmission probabilities of the primary and secondary networks, respectively, versus ν_e^p and ν_e^s.

https://doi.org/10.1017/S1446181117000244 Published online by Cambridge University Press

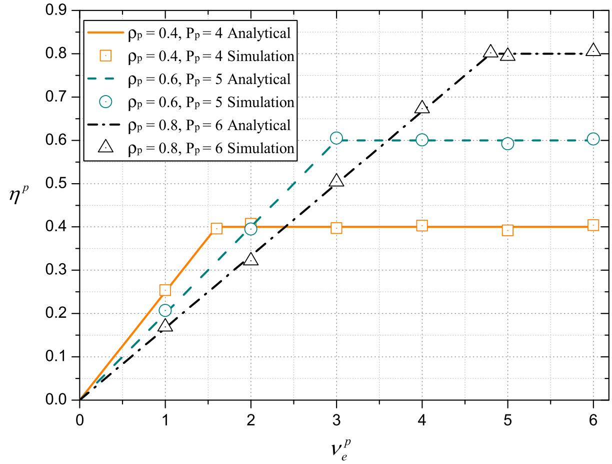

FIGURE 3. Transmission probability of the PTs.

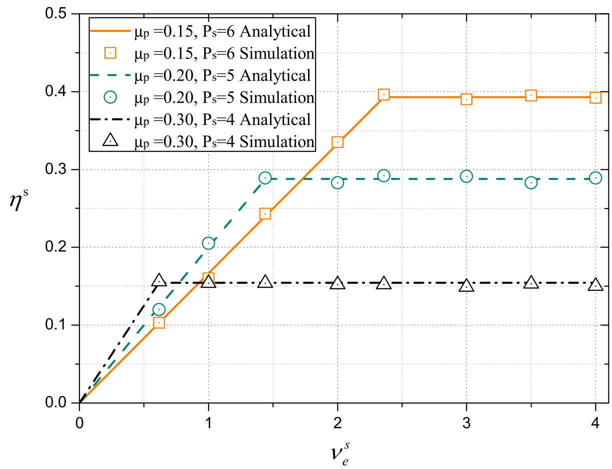

FIGURE 4. Transmission probability of the STs.

We observe that the transmission probabilities of PTs and STs are piecewise functions with respect to v_e^p and v_e^s, which are intuitively expected according to Theorems 3.1 and 3.3; also, the simulation results fit closely to our analytical results.

Figure 5 plots the coverage probability of the primary network. It is observed that the approximated coverage probability of the primary network derived in Theorem 4.3 under Assumption 4.2 is quite accurate. An intuitive explanation of the above observation is that, as mentioned in the articles by Lee and Haenngi [14] and Song et al. [20], the higher-order statistics of the point process formed by the active STs have a

https://doi.org/10.1017/S1446181117000244 Published online by Cambridge University Press

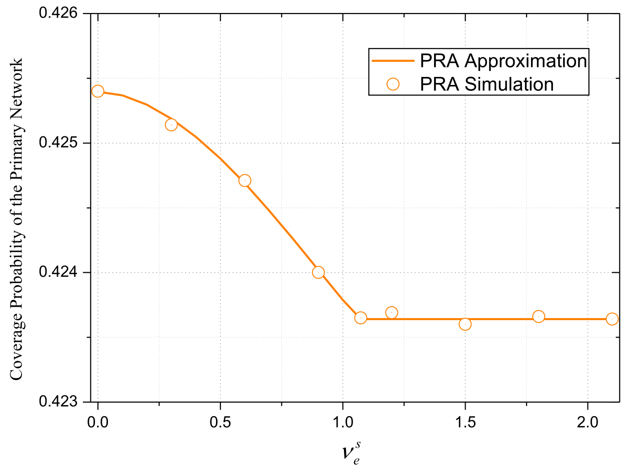

FIGURE 5. Coverage probability of the primary network.

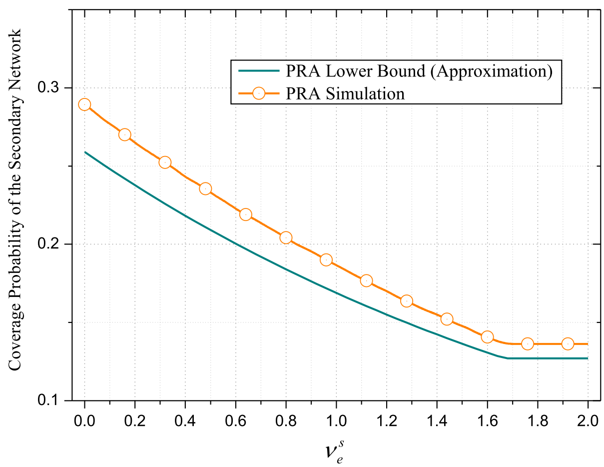

FIGURE 6. Coverage probability of the secondary network.

marginal effect on the computed Laplace transform of the aggregate interference from all active STs to the typical PR at the origin.

Figure 6 plots the analytical results on the coverage probability of the secondary network with the corresponding simulated values. As observed in Figure 6, the lower bound on the coverage probability of the secondary network derived in Theorem 5.6 under Assumption 5.4 is effective.

7. Conclusions

We studied the performance of the large-scale overlay CR networks powered by renewable energy. Upon harvesting sufficient energy, the PTs employ an Aloha-type MAC protocol to access the spectrum with probability ρ_p, while the STs are allowed to access the spectrum, only if the maximum signal power of the received beacons sent from the active primary receivers (PRs) is lower than a certain threshold N_{ra}. By applying tools from random walk theory and stochastic geometry, and assuming an infinite battery capacity for the energy storage module, we characterize the transmission probabilities of PTs and STs, respectively. Based on such results, the coverage probabilities of the primary and secondary networks are analysed. We hope that the results in this paper will provide new insights to the optimal design of the practical overlay CR networks powered by renewable energy.

Acknowledgements

This work was supported in part by the Public Welfare Research Project of Guangdong Province under Grant 2014A010103031, the Fundamental Research Funds for the Central Universities under Grant N150403001, and the National Natural Science Foundation of China under Grant 61671141, U14331156, 1151002, 61401079, 61501038.

Appendix A. Proof of Theorem 3.1

PROOF. We first consider the case of $\nu_e^p/P_p \le \rho_p$. Particularly, for $\nu_e^p/P_p \le \rho_p$, based on equation (3.1), it can be verified that

$$\sum_{t=1}^{n} \mathbb{E}[Z_t^p(\mathbf{x})] = P_p \sum_{t=1}^{n} \mathbb{E}[\mathcal{G}_t^p] + \mathbb{E}[S_t^p(\mathbf{x})],$$

where $\mathcal{G}_t^p$ is defined in equation (2.4). Then, since $\mathbb{E}[S_t^p(\mathbf{x})] \ge 0$,

$$\lim_{n\to\infty} \frac{1}{n} \sum_{t=1}^{n} \mathbb{E}[Z_t^p(\mathbf{x})] \ge P_p \lim_{n\to\infty} \frac{1}{n} \sum_{t=1}^{n} \mathbb{E}[\mathcal{G}_t^p]. \tag{A.1}$$

As such, based on equations (2.1) and (A.1), since

$$\lim_{n\to\infty} \frac{1}{n} \sum_{t=1}^{n} \mathbb{E}[Z_t^p(\mathbf{x})] = \nu_e^p,$$

we obtain an upper bound on η^p as

$$\eta^p \le \frac{\nu_e^p}{P_p}. \tag{A.2}$$

For the lower bound on η^p, based on Huang's work [11], it can be verified that

$$\eta^p \ge \frac{\nu_e^p}{P_p}. \tag{A.3}$$

https://doi.org/10.1017/S1446181117000244 Published online by Cambridge University Press

Then, using equations (A.2)–(A.3) we obtain

$$\eta^p = \frac{\nu_e^p}{P_p}. \tag{A.4}$$

for $\nu_e^p/P_p \leq \rho_p$. We next consider the case of $\nu_e^p/P_p > \rho_p$. Particularly, for $\nu_e^p/P_p > \rho_p$, using equation (2.8), we have

$$\begin{aligned}
\eta^p &= \lim_{n\to\infty} \frac{1}{n} \sum_{t=1}^{n} \mathbb{E}[\mathbf{I}_{S_{t-1}^p(\mathbf{x}) \geq P_p} \cdot \mathcal{X}_t^p] \\
&\overset{(a)}{=} \lim_{n\to\infty} \frac{1}{n} \sum_{t=1}^{n} \mathbb{E}[\mathbf{I}_{S_{t-1}^p(\mathbf{x}) \geq P_p}] \cdot \rho_p \\
&= \lim_{n\to\infty} \frac{1}{n} \sum_{t=1}^{n} P(S_{t-1}^p(\mathbf{x}) \geq P_p)\rho_p,
\end{aligned}$$

where (a) follows from the fact that $\mathbb{E}[\mathcal{X}_t^p] = \rho_p$. Note that

$$S_{t-1}^p(\mathbf{x}) \geq \sum_{j=1}^{t-1} (Z_j^p(\mathbf{x}) - P_p \cdot \mathcal{X}_j^p). \tag{A.5}$$

As such, from equation (A.5), we have

$$\begin{aligned}
P(S_{t-1}^p(\mathbf{x}) \geq P_p) &\geq P\bigg(\sum_{j=1}^{t-1} (Z_j^p(\mathbf{x}) - P_p \cdot \mathcal{X}_j^p) \geq P_p\bigg) \\
&= P\bigg(\frac{t}{t-1} \sum_{j=1}^{t-1} Z_j^p(\mathbf{x}) - \nu_e \geq \xi\bigg),
\end{aligned} \tag{A.6}$$

where

$$\xi = P_p \cdot \bigg(\rho_p - \frac{\nu_e}{P_p} + \bigg(\frac{1}{t-1}\sum_{j=1}^{t-1} \mathcal{X}_j^p - \rho_p\bigg) + \frac{1}{t-1}\bigg).$$

Notice that $\nu_e^p/P_p > \rho_p$. As a result, there exists certain k such that

$$\rho_p - \frac{\nu_e}{P} + \bigg(\frac{1}{t-1}\sum_{j=1}^{t-1} \mathcal{X}_t^p - \rho_p\bigg) + \frac{1}{t-1} < 0$$

for $t-1 \geq k$. Based on this fact, by applying Cantelli's inequality [8], we get

$$P\bigg(\frac{1}{t-1} \sum_{j=1}^{t-1} Z_j^p(\mathbf{x}) - \nu_e \geq \xi\bigg) \geq 1 - \frac{\delta_e^2/(t-1)}{\delta_e^2/(t-1) + \xi^2} \tag{A.7}$$

for $t-1 \geq k$. Let $\bar{k}(n) = o(n)$ denote an increasing function of t with a lower order as

$$\lim_{n\to\infty} \bar{k}(n) = \infty \quad \text{and} \quad \lim_{n\to\infty} \frac{\bar{k}(n)}{n} = 0.$$

https://doi.org/10.1017/S1446181117000244 Published online by Cambridge University Press

Then, based on equations (A.4), (A.6) and (A.7), for $\nu_e^p/P_p > \rho_p$, we obtain

$$\begin{aligned}
\eta^p &\geq \lim_{n\to\infty} \frac{1}{n}\sum_{t=1}^{n}\Big(1 - \frac{\delta_e^2/(t-1)}{\delta_e^2/(t-1)+\xi^2}\Big)\cdot \rho_p \\
&\overset{(a)}{\geq} \lim_{n\to\infty} \frac{1}{n}\sum_{t=\bar{k}(n)}^{n}\Big(1 - \frac{\delta_e^2/(t-1)}{\delta_e^2/(t-1)+\xi^2}\Big)\cdot \rho_p \\
&\overset{(b)}{=} \lim_{n\to\infty} \frac{1}{n}\sum_{t=\bar{k}(n)}^{n}\rho_p \\
&= \lim_{n\to\infty} \frac{n-\bar{k}(n)}{n}\cdot \rho_p \\
&= \rho_p,
\end{aligned} \tag{A.8}$$

where (a) follows from the fact that $\lim_{n\to\infty}\bar{k}(n) \geq k$ and (b) follows from the fact that for $t-1 \geq \bar{k}(n)$,

$$\lim_{t\to\infty} \frac{\delta_e^2/(t-1)}{\delta_e^2/(t-1)+\xi^2} = 0.$$

This completes the proof of upper bound on η^p for $\nu_e^p/P_p > \rho_p$.

For the lower bound on η_p given $\nu_e^p/P_p > \rho_p$, by the axiom of probability, the following inequality holds

$$\eta^p = \lim_{n\to\infty}\frac{1}{n}\sum_{t=1}^{n} P(S_{t-1}^p(\mathbf{x}) \geq P_p)\rho_p \leq \rho_p. \tag{A.9}$$

As such, for $\nu_e^p/P_p > \rho_p$, with equations (A.8) and (A.9), we have

$$\eta_p = \rho_p. \tag{A.10}$$

Based on equations (A.4) and (A.10), equation (3.3) is immediately obtained. This completes the proof of Theorem 3.1. □

Appendix B. Proof of Theorem 4.3

Proof. With the PRA protocol, for a typical PR at the origin, the SIR is given by

$$\mathrm{SIR}_p = \frac{P_p h_0 d_p^{-\alpha}}{\sum_{i\in\Pi_p^t} P_p h_i |\mathbf{X}_i|^{-\alpha} + \sum_{j\in\Pi_s^{ra}} P_s g_j |\mathbf{Y}_j|^{-\alpha}}.$$

Here Π_p^t denotes the set of all active PTs, Π_s^{ra} denotes the set of all active STs, h_0 is the fading channel power coefficient of a typical primary link, h_i is the power coefficient of the fading channel from the ith active PT to the typical PR with $i \in \Pi_p^t$, g_j is the power coefficient of the fading channel from the jth active ST to the typical PR with $j \in \Pi_s^{ra}$, $\mathbf{X}_i$ is the coordinate of the ith active PT and $\mathbf{Y}_j$ is the coordinate of the jth active ST. According to the PRA protocol, at the typical PR, the interference introduced by the

https://doi.org/10.1017/S1446181117000244 Published online by Cambridge University Press

jth active ST is constrained as $P_s g_j |\mathbf{Y}_j|^{-\alpha} \le P_s N_{ra}/P_p$. Thus, under Assumption 4.2, the coverage probability of the primary network with the PRA protocol is given by

$$\begin{aligned}
\tau_p^{ra} &= P\bigg\{\mathrm{SIR}_p \ge \theta_p \bigg| g_j|\mathbf{Y}_j|^{-\alpha} \le \frac{N_{ra}}{P_p}\bigg\} \\
&= P\bigg\{\frac{P_p h_0 d_p^{-\alpha}}{\sum_{i\in\Pi_p^t} P_p h_i |\mathbf{X}_i|^{-\alpha} + \sum_{j\in\Pi_s^{ra}} P_s g_j |\mathbf{Y}_j|^{-\alpha}} \ge \theta_p \bigg| g_j|\mathbf{Y}_j|^{-\alpha} \le \frac{N_{ra}}{P_p}\bigg\} \\
&= \mathbb{E}_{\mathbf{X}}\bigg[\prod_{i\in\Pi_p^t} \mathbb{E}_h[e^{-(\theta_p h_i |\mathbf{X}_i|^{-\alpha})/d_p^{-\alpha}}]\bigg] \times \mathbb{E}_{\mathbf{Y}}\bigg[\prod_{j\in\Pi_s^{ra}} \mathbb{E}_g\bigg[e^{-(\theta_p P_s g_j |\mathbf{Y}_j|^{-\alpha})/P_p d_p^{-\alpha}} \bigg| g_j \le \frac{N_{ra}|\mathbf{Y}_j|^{\alpha}}{P_p}\bigg]\bigg] \\
&\overset{(a)}{=} \exp\bigg\{-\frac{2\pi^2}{\alpha\sin(2\pi/\alpha)}\mu_p \theta_p^{2/\alpha} d_p^2\bigg\} \\
&\quad \times \exp\bigg\{-2\pi\int_0^\infty \bigg(1 - \int_0^{N_{ra}u^\alpha/P_p} e^{-(\theta_p P_s g u^{-\alpha})/P_p d_p^{-\alpha}} \times \frac{e^{-g}}{1-e^{-(N_{ra}u^\alpha)/P_p}}\,dg\bigg)\lambda_{ra}^{\mathbf{R}}(u)u\,du\bigg\} \\
&\overset{(b)}{=} \exp\bigg\{-\frac{2\pi^2}{\alpha\sin(2\pi/\alpha)}\theta_p^{2/\alpha} d_p^2 \mu_p\bigg\} \times \exp\bigg\{-2\pi\lambda_0 Q_{ra}\int_0^\zeta (1-\varrho(u))\mathcal{P}(u)u\,du\bigg\} \\
&\quad \times \exp\bigg\{-2\pi\lambda_0 \frac{\nu_e^s}{P}\int_\zeta^\infty (1-\varrho(u))u\,du\bigg\},
\end{aligned}$$

where (a) follows from the fact that the probability density function of g conditioned on $g \le t$ is given by

$$f(g \mid g \le t) = \frac{e^{-g}}{1-e^{-t}},$$

and (b) follows from equation (3.5). This completes the proof of Theorem 4.3. □

References

[1] F. Baccelli and B. Blaszczyszyn, *Stochastic geometry and wireless networks*, Volume 1 (Now Publishers Inc, Boston, MA, 2010); doi:10.1561/1300000006.

[2] F. Baccelli, B. Blaszczyszyn and P. Muhlethaler, "Stochastic analysis of spatial and opportunistic aloha", *IEEE J. Sel. Areas Commun.* **27** (2009) 1105–1119; doi:10.1109/JSAC.2009.090908.

[3] W. Chung, S. Park, S. Lim and D. Hong, "Spectrum sensing optimization for energy-harvesting cognitive radio systems", *IEEE Trans. Wirel. Commun.* **13** (2014) 2601–2613; doi:10.1109/TWC.2014.032514.130637.

[4] O. Ellabban, H. Abu-Rub and F. Blaabjerg, "Renewable energy resources: current status, future prospects and their enabling technology", *Renew. Sustainable Energy Rev.* **39** (2014) 748–764; doi:10.1016/j.rser.2014.07.113.

[5] R. G. Gallager, *Stochastic processes: theory for applications* (Cambridge University Press, UK, 2013), https://pdfs.semanticscholar.org/2152/c76ba0b6e30f990b52572d6cfc204af9c619.pdf.

[6] D. Gunduz, K. Stamatiou, N. Michelusi and M. Zorzi, "Designing intelligent energy harvesting communication systems", *IEEE Commun. Mag.* **52** (2014) 210–216; doi:10.1109/mcom.2014.6710085.

[7] M. Haenggi, J. G. Andrews, F. Baccelli, O. Dousse and M. Franceschetti, "Stochastic geometry and random graphs for the analysis and design of wireless networks", *IEEE J. Sel. Areas Commun.* **27** (2009) 1029–1046; doi:10.1109/jsac.2009.090902.

[8] Y. Haimes, *Research and practice in multiple criteria decision making: Proc. XIVth Int. Conf. on Multiple Criteria Decision Making (MCDM) Charlottesville,* Virginia, USA, 1998, Volume of 487 *Lecture Notes in Economics and Mathematical Systems* (Springer, Berlin–Heidelberg, 2000); doi:10.1007/978-3-642-57311-8.

[9] T. Han and N. Ansari, "Powering mobile networks with green energy", *IEEE Wirel. Commun.* **21** (2014) 90–96; doi:10.1109/mwc.2014.6757901.

[10] Z. Hasan, H. Boostanimehr and V. K. Bhargava, "Green cellular networks: a survey, some research issues and challenges", *IEEE Commun. Surv. Tutor.* **13** (2011) 524–540; doi:10.1109/surv.2011.092311.00031.

[11] K. Huang, "Spatial throughput of mobile ad hoc networks powered by energy harvesting", *IEEE Trans. Inf. Theory* **59** (2013) 7597–7612; doi:10.1109/TIT.2013.2276811.

[12] A. Kwasinski and A. Kwasinski, "Increasing sustainability and resiliency of cellular network infrastructure by harvesting renewable energy", *IEEE Commun. Mag.* **53** (2015) 110–116; doi:10.1109/mcom.2015.7081083.

[13] J. Lee, J. G. Andrews and D. Hong, "The effect of interference cancellation on spectrum-sharing transmission capacity", in: *IEEE International Conference on Communications (ICC)* (IEEE, Kyoto, Japan, 2011) 1–5; doi:10.1109/icc.2011.5963391.

[14] C.-h. Lee and M. Haenggi, "Interference and outage in Poisson cognitive networks", *IEEE Trans. Wirel. Commun.* **11** (2012) 1392–1401; doi:10.1109/twc.2012.021512.110131.

[15] S. Lee, R. Zhang and K. Huang, "Opportunistic wireless energy harvesting in cognitive radio networks", *IEEE Trans. Wirel. Commun.* **12** (2013) 4788–4799; doi:10.1109/twc.2013.072613.130323.

[16] N. Pappas, J. Jeon, A. Ephremides and A. Traganitis, "Optimal utilization of a cognitive shared channel with a rechargeable primary source node", *J. Commun. Netw.* **14** (2012) 162–168; doi:10.1109/itw.2011.6089526.

[17] S. Park and D. Hong, "Achievable throughput of energy harvesting cognitive radio networks", *IEEE Trans. Wirel. Commun.* **13** (2014) 1010–1022; doi:10.1109/twc.2013.121713.130820.

[18] S. Park, S. Lee, B. Kim, D. Hong and J. Lee, "Energy-efficient opportunistic spectrum access in cognitive radio networks with energy harvesting", in: *Proceedings of the 4th international conference on cognitive radio and advanced spectrum management* Barcelona, Spain (ACM, New York, 2011) 62, 1–5; https://pdfs.semanticscholar.org/7359/2aa42bfc4f9d69b4a300049f46bd330ed628.pdf.

[19] J. Proakis, *Digital communications* (McGraw-Hill, New York, 1995).

[20] X. Song, C. Yin, D. Liu and R. Zhang, "Spatial throughput characterization in cognitive radio networks with threshold-based opportunistic spectrum access", *IEEE J. Sel. Areas Commun.* **32** (2014) 2190–2204; doi:10.1109/JSAC.2014.1411RP05.

[21] D. Stoyan, W. S. Kendall and J. Mecke, "Stochastic geometry and its applications", in: *Wiley series in probability and mathematical statistics* (Wiley, Chichester, W. Sussex, New York, 1987). Rev. translation of: stochastische geometrie; doi:10.1002/9781118658222.

[22] R. Tandra, S. M. Mishra and A. Sahai, "What is a spectrum hole and what does it take to recognize one?", *Proc. IEEE* **97** (2009) 824–848; doi:10.1109/JPROC.2009.2015710.

[23] R. Vaze, "Transmission capacity of spectrum sharing ad hoc networks with multiple antennas", *IEEE Trans. Wirel. Commun.* **10** (2011) 2334–2340; doi:10.1109/wiopt.2011.5930039.

[24] X. Wang, M. Chen, T. Taleb, A. Ksentini and V. C. Leung, "Cache in the air: exploiting content caching and delivery techniques for 5g systems", *IEEE Commun. Mag.* **52** (2014) 131–139; doi:10.1109/mcom.2014.6736753.

[25] B. Wang and K. R. Liu, "Advances in cognitive radio networks: a survey", *IEEE J. Sel. Top. Signal Process.* **5** (2011) 5–23; doi:10.1109/JSTSP.2010.2093210.

[26] S. Weber, J. G. Andrews and N. Jindal, "The effect of fading, channel inversion, and threshold scheduling on ad hoc networks", *IEEE Trans. Inf. Theory* **53** (2007) 4127–4149; doi:10.1109/TIT.2007.907482.

[27] S. Yin, Z. Qu and S. Li, "Achievable throughput optimization in energy harvesting cognitive radio systems", *IEEE J. Sel. Areas Commun.* **33** (2015) 407–422; doi:10.1109/JSAC.2015.2391712.

[28] S. Yin, E. Zhang, Z. Qu, L. Yin and S. Li, “Optimal cooperation strategy in cognitive radio systems with energy harvesting”, *IEEE Trans. Wirel. Commun.* **13** (2014) 4693–4707; doi:10.1109/TWC.2014.2322972.

[29] Y. Zeng, Y.-C. Liang, A. T. Hoang and R. Zhang, “A review on spectrum sensing for cognitive radio: challenges and solutions”, *EURASIP J. Adv. Signal Process.* **2010** (2010) 381–465; doi:10.1109/COMST.2016.2631080.

[30] H. Zhang, C. Jiang, N. C. Beaulieu, X. Chu, X. Wang and T. Q. Quek, “Resource allocation for cognitive small cell networks: a cooperative bargaining game theoretic approach”, *IEEE Trans. Wirel. Commun.* **14** (2015) 3481–3493; doi:10.1109/TWC.2015.2407355.

[31] Q. Zhao and B. M. Sadler, “A survey of dynamic spectrum access”, *IEEE Signal Proc. Mag.* **24** (2007) 79–89; doi:10.1109/msp.2007.361604.

[32] X. Zhao, C. Yang, Y. Yao, Z. Chen and B. Xia, “Cognitive and cache-enabled d2d communications in cellular networks”, Preprint, 2015, arXiv:1510.06480.